Journal of Applied Polymer Science

REVIEW

The organic electrochemical transistor for biological applications

Xenofon Strakosas, Manuelle Bongo, Róisín M. Owens

Department of Bioelectronics, Ecole Nationale Supérieure des Mines CMP-EMSE, MOC, 880 avenue de Mimet, 13541, Gardanne, France

Xenofon Strakosas and Manuelle Bongo contributed equally to this work.

Correspondence to: R. M. Owens (E-mail: owens@emse.fr)

ABSTRACT: The rising field of bioelectronics, which couples the realms of electronics and biology, holds huge potential for the development of novel biomedical devices for therapeutics and diagnostics. Organic electronic devices are particularly promising; the use of robust organic electronic materials provides an ideal biointerface due to their reported biocompatibility, and mechanical matching between the sensor element and the biological environment, are amongst the advantages unique to this class of materials. One promising device emerging from this field is the organic electrochemical transistor (OECT). Arguably, the most important feature of an OECT is that it provides local amplification and as such can be used as a high fidelity transducer of biological events. Additionally, the OECT combines properties and characteristics that can be tuned for a wide spectrum of biological applications. Here, we frame the development of the OECT with respect to its underlying optimization for a variety of different applications, including ion sensing, enzymatic sensing, and electrophysiology. These applications have allowed the development of OECTs to sense local ionic/biomolecular and single cell activity, as well characterization of tissue and even monitoring of function of whole organs. The body of work reviewed here demonstrates that the OECT is an extremely versatile device that emerges as an important player for therapeutics and diagnostics. © 2015 Wiley Periodicals, Inc. J. Appl. Polym. Sci. **2015**, *132*, 41735.

KEYWORDS: biosensing; organic bioelectronics; organic electrochemical transistor; PEDOT:PSS

Received 3 October 2014; accepted 13 November 2014

DOI: 10.1002/app.41735

INTRODUCTION

The coupling of organic electronics with biology is an emerging and continuously growing field.[1] The motivation for organic bioelectronics is to address and anticipate the current and future diagnostic and therapeutic needs of the biomedical community.[2,3] These needs include detecting low concentrations of biological analytes, low amplitude brain activity, and pathogens, as well as improving compatibility with the biological environment.[4] Electrical methods for biological sensing are considered advantageous, in particular due to the fact that they are label-free, and do not require expensive and time consuming techniques involving fluorophores or chromophores (optical methods). Current diagnostic approaches using electrical sensors involve electrochemical biosensors, passive metal electrodes, and/or large scale integrated systems, in which the operating principle is based on redox reactions, changes in the local potential or impedance. However, for electrochemical sensors and passive recording sites for electrophysiology the biological signals are often challenging to record and require further amplification to become detectable, necessitating a push toward more active, sensitive, and biocompatible devices.[5,6] A promising technology that has the potential to overcome such limitations and respond to these specific requirements is the organic electrochemical transistor (OECT).

The OECT, first reported by White *et al.*,[7] is a three terminal device in a transistor configuration (source, gate, and drain) [Figure 1(a)]. The source and drain are connected by an organic conducting material in which an electronic current is generated (I_d) in response to a potential difference. A variable potential at the gate controls the magnitude of the drain current (I_d) by doping and dedoping the channel.

The OECT belongs to a broader class of transistors called electrolyte gated transistors (EGTs), in which the electrolyte is an integral part of the device.[10] This property makes the EGT compatible with aqueous environments. Apart from OECTs, a major subclass of the EGT is the electrolyte gated organic field effect transistor (EGOFET),[11] which has also been used as a diagnostic tool.[12–14] The difference between OECTs and EGOFETs lies in the interface between the channel and the electrolyte.[15] Specifically, in EGOFETs the ions of the electrolyte create an electrical double layer (EDL) with the charges (electrons/holes) of the

Xenofon Strakosas received his BS degree in Physics in 2008, and his Master's degree in Nanosciences and Nanotechnologies in 2011, both from the Aristotle University of Thessaloniki, Greece. He is a PhD student in the Department of Bioelectronics (BEL) at the Centre Microélectronique de Provence of the Ecole Nationale Supérieure des Mines de Saint-Étienne. He is interested in organic electrochemical transistors and their functionalization with various biorecognition elements for use as biosensors.

Manuelle Bongo received a Licence degree in Biology from Burgundy University, and subsequently completed a Master degree in biology and healthcare in 2008. She has just completed her PhD in the Department of Bioelectronics (BEL) at the Centre Microélectronique de Provence of the Ecole Nationale Supérieure des Mines de Saint-Étienne. The topic of her thesis was the the development of an *in vitro* blood-brain barrier model integrated with the OECT.

Róisín M. Owens is an Associate Professor in the Department of Bioelectronics at the Centre Microélectronique de Provence. She received her BA in Biochemistry at Trinity College Dublin, and her PhD in Biochemistry and Molecular Biology at Southampton University. Her current research centers on application of organic electronic materials for diagnostics *in vitro*. She has received several awards including the European Research Council starting grant, a Marie Curie fellowship, and an EMBO fellowship.

channel. In contrast, in OECTs, ions from the electrolyte can penetrate the whole bulk of the polymeric channel. This key difference enables the OECT to exhibit high amplification properties in subvolt operation regimes, preventing electrolysis, and extending operating times necessary for *in-vitro* and *in-vivo* applications.[8] The latter affords high sensitivity sensing for a wide spectrum of applications without additional amplification.

The OECT offers a unique set of advantages for biomedical tools. One notable advantage includes adaptability to a wide variety of fabrication methods, from simple to complex; OECTs have been fabricated using low-cost printing techniques, high current modulation,[16–20] and fast response.[21] OECTs exhibit high stability in aqueous solutions and in one example showed reproducible, reliable performance when maintained in cell culture media under physiological conditions for 5 weeks.[22] Simple, planar, all PEDOT:PSS transistors on the macroscale have been shown to be capable of detecting glucose levels that exist in human saliva.[23,24] For more challenging applications, OECTs are equally compatible with ongoing miniaturization techniques to the microscale, necessitated for the fabrication of high density electrode arrays for better interfacing with single neurons,[25,26] integration with microfluidics for detection of multiple analytes,[27,28] and lab on chip technologies.[28] The use of robust and versatile organic materials has also facilitated the fabrication of conformal OECTs [Figure 2(a)] for noninvasive, long term, and continuous recordings.[29] Additionally, OECTs have been integrated with natural and synthetic fibers for fully integrated sensors and wearable circuits compatible with human

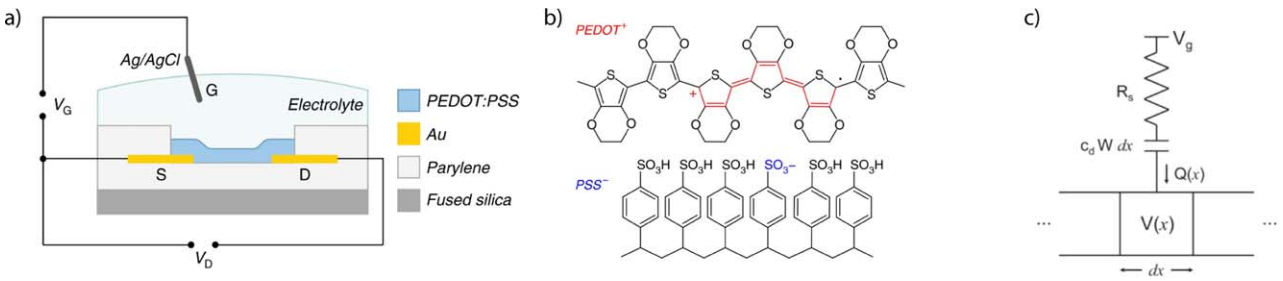

Figure 1. The OECT: a. Schematic cross-section of an OECT, b. PEDOT:PSS structure. (a, b reproduced from [8], with permission from [Nature Publishing Group]). c. Ionic circuit of an OECT (c reproduced from [9], with permission from [Wiley-VCH]). [Color figure can be viewed in the online issue, which is available at wileyonlinelibrary.com.]

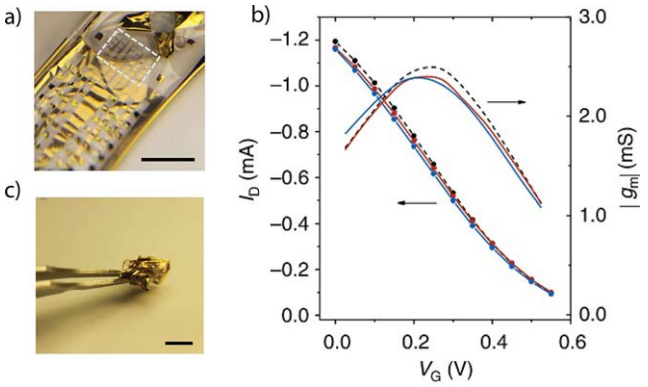

Figure 2. Robust micrometer scale, high amplification OECTs: a. An array of OECTs on a thin flexible substrate: scale bar = 1 cm, b. the array is extensively crumpled, c. (left axis) transfer characteristics of device before (red) and after (blue) crumpling (right axis) transconductance and time response for devices before (red) and after (blue) crumpling. (a, b, c reproduced from [8], with permission from [Nature Publishing Group]). [Color figure can be viewed in the online issue, which is available at wileyonlinelibrary.com.]

skin.[30–32] All OECTs reported to date have been fabricated with conducting polymers (CPs), as the active material in the channel due to their highly desirable properties, as discussed below.

CPs, first discovered in 1976 by Alan MacDiarmid, Hideki Shirakawa, and Alan Heeger, exhibit a wide spectrum of desired characteristics.[33,34] Of particular interest to biomedical applications, they exhibit mixed conductivity; ionic and electronic. Some of the first applications of CPs in the biomedical arena were their use as coatings on metal electrodes, where they were shown to improve recordings of brain activity by lowering the impedance of the electrode.[14,25] CPs are chemically tuneable, and can be designed according to the needs of each application. For instance, CPs have been designed to entrap enzymes and mediators.[35,36] Direct wiring of the active site of enzymes to electrodes has been explored, using polyelectrolytes with redox active groups, and CPs.[37–39] Electrochemical biosensors have enlisted these types of CPs to improve stability and sensitivity. Finally, CPs have been shown repeatedly to be biocompatible, hosting a wide variety of cell types.[4,40] Part of their compatibility with live cells is most likely due to the fact that these polymeric materials contain no broken bonds and are oxide-free, resulting in a closer interaction with cells hosted on their surface, possibly facilitating adhesion and promoting ionic interactions.[40–43] This concept has been extensively discussed by Rivnay and co-authors and is key to the understanding that CPs work well in electrolytes and, unlike other devices with semi-CPs, are not isolated from the sensing events taking place in the aqueous milieu.[40] Other advantages of CPs that will be highlighted below include their optical transparency and their mechanical flexibility akin to tissue, providing benefits for tissue engineering.

A well-studied and widely used CP is poly(3,4-ethylenedioxythiophene) doped with poly(styrene sulfonate) (PEDOT:PSS). PEDOT:PSS is a *p*-type CP, in which the negative charge of PSS is compensated by a hole in the PEDOT backbone [Figure 1(b)]. This CP exhibits high electronic conductivities, with typical conductivity values of commercially available PEDOT:PSS reaching approximately 1000 S/cm. Cross-linking of PEDOT:PSS with a silane (GOPS; 3-glycidoxypropyltrimethoxysilane) is a frequently used strategy for improving adhesion of PEDOT:PSS with substrates, and preventing delamination in aqueous milieux.[8,13] The conductivity of PEDOT:PSS drops with the addition of the cross-linker, however, conductivity measured after the addition of the crosslinker is in the order of 300 S/cm, adequate for biological applications. Such cross-linked PEDOT:PSS films have been shown to swell in aqueous solutions, although to a lesser extent than uncross-linked films, speaking to their "hydrogel" type nature and implying their compatibility with electrolyte solutions. Furthermore, PEDOT:PSS shows high ionic conductivities: ionic mobilities for small ions migrating in PEDOT:PSS can reach values that exist in dilute electrolytes.[44] Indeed, a novel class of devices based on PEDOT:PSS have been reported, which have ions as their main charge carrier (Iontronics), with subsequent development of ion transistors and ion pumps demonstrated for delivery of ions, neurotransmitters, and other small molecules.[45–47] The combined high ionic and electronic mobilities are key reasons for PEDOT:PSS emerging as the champion material for devices such as OECTs.

Apart from choosing the optimal materials for an OECT, it is important to understand its operating principle. Bernards and Malliaras,[9] have reproduced the transient behavior, the speed with which the transistor responds to external changes such as biological signals, and the steady state behavior of an OECT by modeling it as an ionic and electronic circuit [Figure 1(c)]. The electronic circuit refers to the current of holes inside the channel and the changes of its magnitude on dedoping. The ionic circuit [Figure 1(c)], has been modeled as a capacitor and resistor in series. For simplicity, the capacitance of the gate has been neglected. The resistor in the model refers to the ionic strength of the electrolyte and the capacitor, to the amount of ions that can be stored in the bulk of the channel. The model explains the operating principle of the OECT which is affected by the interplay between the ionic and electronic currents. Thus, an understanding of the parameters that influence these properties must be taken into consideration and tuned according to the specific applications at hand. These parameters include: the material/size of the gate, the resistance of the electrolyte, and the size and geometry of the channel. Once defined, optimal parameters must be weighed against considerations such as fabrication–for instance; micrometer scale transistors exhibit fast responses which are stable for higher frequencies, making them suitable and more specific for fast biological events (such as neuronal signaling), however, scaling down the dimensions requires somewhat complex lithographic techniques [Figure 2(a)].

Arguably, the most important device property of the OECT is related to its amplification properties. High amplification is a common necessity for unraveling biological information; to increase signal to noise ratio and to lower detection limits thus increasing sensitivity. For example, in electrophysiology it is important to record brain activity that has a wide spectrum of frequencies and amplitudes. For example, the amplitude of an action potential is on the order of a few microvolts, and by

taking advantage of its inherent transistor properties, OECTs can be used to locally amplify the signal.[22] The efficiency of the amplification can be measured by the transconductance, which is defined as $g_m = \frac{\Delta I_d}{\Delta V_g}$. Therefore, the higher the value of the transconductance, the better the gain. Khodagholy *et al.*,[8] have shown that the OECT reaches transconductance values in the milliSiemens range, outperforming traditional and other organic transistors [Figure 2(b)], an impressive feat for a device fabricated with solution processed materials at room temperature. Furthermore, as shown in Figure 2(b,c), the transconductance and the time characteristics are not affected even after extensive use and harsh manipulation. Finally, by carefully selecting and varying geometrical characteristics such as channel length, width and thickness, Rivnay *et al.*,[48] have engineered OECTs with peak transconductance values at zero gate voltage. This is of importance in many applications where very low voltages are required, for example, when cell or lipid bilayer integrity has to be maintained over an extended period of biasing.[49] Moreover, omitting additional biasing facilitates simple integration with circuits and recording systems, something desirable for lab on chip applications. From the above, we see how individual properties and characteristics of an OECT may be tuned for a broad range of biological applications.

APPLICATIONS IN BIOLOGY

OECTs Coupled with Biological Moieties for Sensing

In this section, work related to the coupling of OECTs with a variety of different biological molecules and macromolecules will be discussed, including ions, proteins (enzymes and antibodies), lipids, and nucleic acids. These devices have been reported for applications in basic research but particularly as new alternatives for low-cost diagnostics.

OECTs as Ion Sensors

The electrolyte is an integral part of an OECT; variations in its ionic concentration affect the device properties. Therefore, sensing of ions, which is of great importance in healthcare diagnostics, has been possible with the OECT. Lin *et al.*,[50] have shown that altering the ionic concentration of an electrolyte affects its channel current (I_d). Figure 3(a) shows a transfer curve, which is a function of the drain current with respect to the sweep of the gate voltage, for a range of concentrations of a potassium chloride (KCl) electrolyte. The transfer characteristics display the decrease in I_d with increase of the V_g, with a shift of these curves to lower values of V_g, when the ionic concentration increases. This behavior can be simply explained from the ionic circuit in Figure 1(c); the higher the ionic concentration in the electrolyte the higher the ionic charge at the interface with PEDOT:PSS. So, the increase of the charge shifts the effective gate voltage ($V_{g,eff}$) (constituting the potential drop to the channel) to higher values and in turns dedopes the channel. Apart from changes in electrolyte concentration, changes in electrolyte composition can shift the $V_{g,eff}$ in the OECT, a principle used by Tarabella *et al.*,[53,54] for sensing liposomes and micelle formation of cetyltrimethylammonium bromide.

Svensson *et al.*,[51] have integrated OECTs in circuits for ion sensing to improve the sensitivity. In this case, two transistors were connected with two resistors in a Wheatstone bridge circuit configuration [Figure 3(b)]. After application of a small constant drain voltage the transistors operate in a resistive mode and the potential difference (V_{diff}) between the two transistors is continuously recorded. By additional application of a sinusoidal gate voltage of 10 Hz, a change of the resistance in the electrolyte and thus, the V_{diff} can be measured. When the ionic concentration of the electrolyte in both transistors is the same, no potential difference is observed. By changing, however, the concentration of the electrolyte in the second transistor, a potential difference is observed. In Figure 3(c) (inset; raw data), we see how the phase of the potential between the two transistors shifts versus the concentration difference in the two electrolytes.

The importance of sensing specific ions has prompted the development of ion-selective OECT sensors (IS-OECT). Sessolo *et al.*,[52] as well as Mousavi *et al.*,[55] have combined OECTs with polymeric membranes that permit the passage of specific ions. In Figure 3(d), the lay-out of an ion-selective OECT is shown. Briefly, a polyvinylchloride-based potassium-selective membrane was placed between a gel electrolyte and the electrolyte of interest, separating the channel from the gate of the OECT. By increasing the concentration of the electrolyte, a decrease in the drain current which is proportional to the $[K^+]$ is observed. This is attributed to the increase number of K^+ ions penetrating the channel and dedoping it, or to the decrease of the electrolyte resistance. Figure 3(e) shows the calibration curve of drain current and effective membrane voltage versus ion concentration for pure KCl and NaCl solutions. The sensitivity to K^+ ions is an order of magnitude higher than that of Na^+ ions, and this confirms the ion selectivity of the membrane. In a similar configuration, Bernards *et al.*,[49] have placed a lipid bilayer with and without embedded proteins, in this case, bacterial gramicidin ion pores, selective for monovalent cations, comprise a selective protein based membrane instead of a polymeric one. In the absence of gramicidin no I_d modulation was observed when a gate potential was applied, whereas, in the presence of gramicidin channels a clear modulation was observed although only in the presence of KCl, not in the presence of $CaCl_2$, demonstrating the selectivity of the gramicidin ion pore towards monovalent cations. A 1V pulse was demonstrated to disrupt the bilayer membrane, underlying the importance of operation at low voltages when interfacing with biological systems.

OECTs as Enzymatic Sensors

One of the first applications of the OECT for interfacing with biology was as an enzymatic sensor.[56] The operating principle of an OECT enzymatic sensor involves either a change in a local pH on oxidation of species or transfer of electrons to the gate of the device [Figure 4(a)]. By measuring changes in pH Nishizawa *et al.*, have used polypyrrole-based OECTs to sense penicillin.[60] They immobilized the enzyme penicillinase which catalyses the turnover of penicillin to penicilloic acid, on top of the channel and on oxidation of the penicillin to peniciloic acid; the change of the local pH increased the conductivity of the polypyrrole. A major drawback, however, is that the conductivity of polypyrrole drops in physiological conditions, creating a mismatch between the device's operation regime and the optimal physiological environment of enzymes and proteins. In contrast, by measuring electron transfer, Zhu *et al.*,[61] demonstrated the use of a PEDOT:

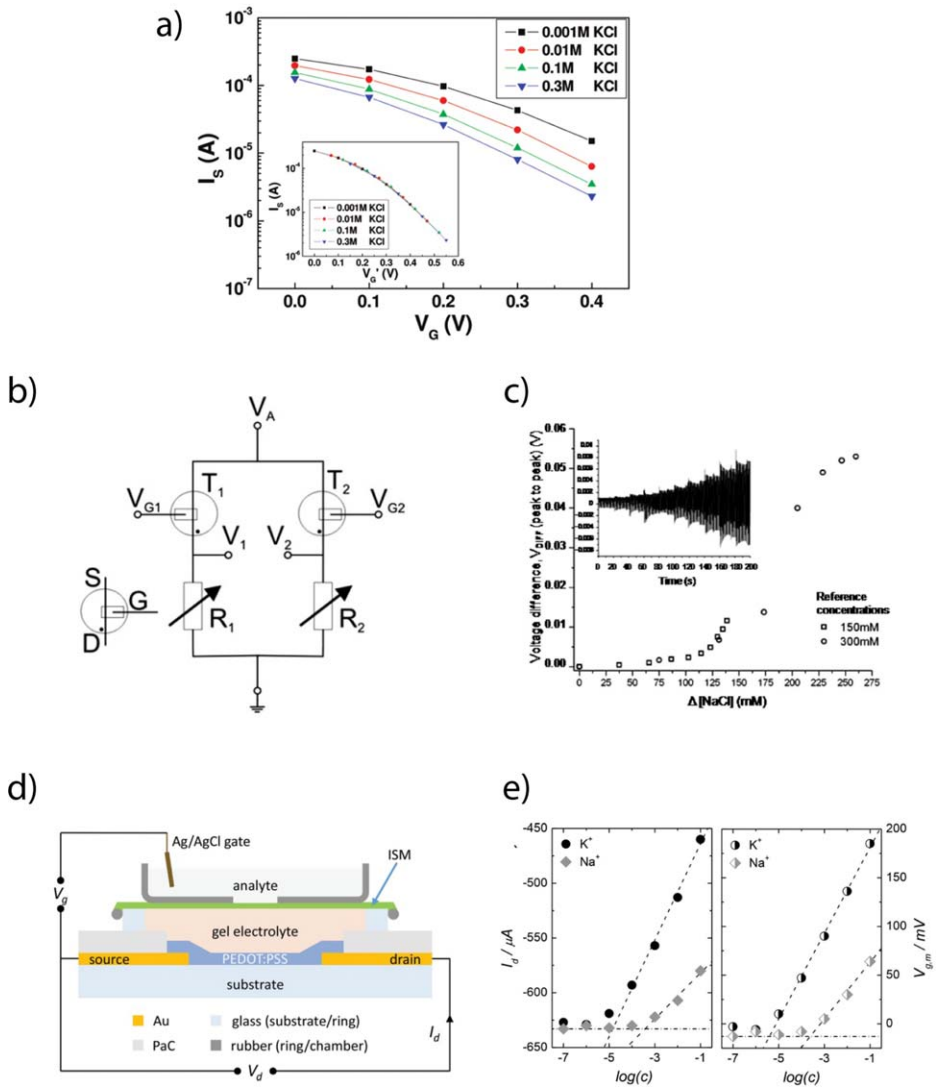

Figure 3. OECTs used as ion sensors: a. Transfer characteristics of an OECT for different concentrations of KCl solutions ($V_d = -0.1$ V). (reproduced from [50], with permission from [ACS Publications]). b. Wheatstone bridge circuit diagram. c. The peak-to-peak voltage difference as a function of concentration difference of NaCl solution, inset curve shows the raw data. (b, c reproduced from [51], with permission from [American Institute of Physics]). d. Schematic of Ion-selective OECT. e. Calibration curves (I_d, $V_{g,m}$ vs. concentration) of pure KCl and NaCl solutions performed using ion selective OECT (IS-OECT). (d, e reproduced from [52], with permission from [Wiley Online Library]). [Color figure can be viewed in the online issue, which is available at wileyonlinelibrary.com.]

PSS-based OECT for glucose sensing in a wide range of pH environments. The sensing mechanism is as follows: glucose oxidase catalyzes the conversion of glucose to gluconolactone in the presence of oxygen, forming hydrogen peroxide (H_2O_2) as a byproduct. The H_2O_2 in turn transfers an electron to the gate of the OECT [Figure 4(a(i))]. In order for charge neutrality to be maintained in the electrolyte, a positive ion penetrates the OECT and compensates the PSS anion [Figure 4(a(ii))], which in turn causes a shift of the $V_{g,eff}$ and thus, a decrease of the source–drain current, logarithmically proportional to the glucose concentration.[62] Pt has been extensively used as a gate in OECT-based glucose sensors[63] because of its good catalytic performance for the oxidation and reduction of H_2O_2 and other biomolecules of interest such as dopamine and adrenaline.[64–66] The sensitivity of OECT devices, after optimization, can detect levels of glucose that exist in human saliva (as low as 8 μM), and sweat (~150 μM), and have been proposed as noninvasive measurement systems.[63]

The geometry of an OECT-based enzymatic sensor affect its sensitivity and a systematic study has been performed by Cicoira *et al.*,[57] who measured the decomposition of H_2O_2, mentioned above as the byproduct of an enzymatic reaction, for devices with a constant channel area, but changing gate area [Figure 4(b)]. They showed that the sensitivity of the device increased as the gate size decreased. Such optimization is confirmed by modeling the behavior of the OECT and optimizing it for two types of applications: for electrochemical sensing and for ion to electron conversion.[67,68] This can be explained by the potential drop at the two interfaces: the gate/electrolyte and

electrolyte/channel interface, respectively, [Figure 4(b)]. Redox active molecules like H_2O_2 which are produced in redox enzymatic reactions, modulate the potential drop at the metal gate/electrolyte interface. In the case of a gate electrode which is much larger than the OECT channel, the potential drop vanishes at this interface as the overall electrode impedance is minimized, and electrochemical potential modulation cannot be detected. In case of smaller gate areas, the potential drop is maximized at the gate/electrolyte interface. In this situation, changes in the potential drop at the gate/electrolyte interface directly affect also the electrolyte/channel interface and thus, modulate the OECT current.

The inherent amplification afforded by the OECT coupled with the optimization of the geometrical characteristics have resulted in highly sensitive enzymatic sensors. However, further modification of the gate with novel materials, such as Pt nanoparticles, has pushed the limit of detection to the nanomolar range. Tang *et al.*,[58] modified a Pt gate with Pt nanoparticles (Pt–NPs) and carbon nanotubes [Figure 4(c)]. Moreover, the enzyme was entrapped on the gate by a chitosan membrane. Owing to their high electrocatalytic activity and the high surface to volume ratio, the Pt–NP modified gate showed an increased sensitivity compared to the pristine Pt gate and the gate modified with carbon nanotubes, and increased the limit of detection for glucose to 10 nM [Figure 4(d)]. Using the same concept, Liao *et al.*,[69] used graphene and reduced graphene oxide flakes at the gate and pushed the sensitivity to a similar range while simultaneously improving the selectivity of sensing by adding a Nafion membrane. Negatively charged acids, such as ascorbic acid and uric acid commonly found in biological media, create interference in the measurements by direct oxidation at the gate. However, the use of a Nafion/chitosan membrane functionalization can repel and attract, respectively, these species while the neutral hydrogen peroxide can diffuse to the gate unimpeded. Finally, Kergoat *et al.*,[70] have blended Pt nanoparticles with PEDOT:PSS. Using the modified PEDOT:PSS:Pt-NPs, they have successfully fabricated OECTs to sense glutamate and acetylcholine, which are important neurotransmitters.

Apart from high sensitivity, the need for low cost and stable biosensors requires the use of alternative materials and simple fabrication techniques. Toward that goal, Shim *et al.*,[23] developed an all-PEDOT:PSS OECT for glucose sensing. PEDOT:PSS, however, exhibits low catalytic properties for the oxidation of H_2O_2. Therefore, owing to its low redox potential, ferrocene has been used as a mediator for the transfer of electrons to the gate. This facilitates a single step fabrication of low cost OECT-based enzymatic sensors. Yang *et al.*,[24] have successfully demonstrated an all plastic OECT glucose sensor using room temperature ionic liquids (RTILs) as an electrolyte, thus solving issues related to long term stability of the OECTs for use in biosensing. Liquid electrolytes are unstable for long term applications, since they are susceptible to evaporation, and thus destabilization of ionic concentration. RTILs, molten salts at room temperature, have gained significant attention in electrochemistry as alternatives to aqueous electrolytes.[71] This is due to their desired characteristics, such as wide electrochemical window of operation, high ionic strength, low or zero evaporation rates, and for biological applications stabilization

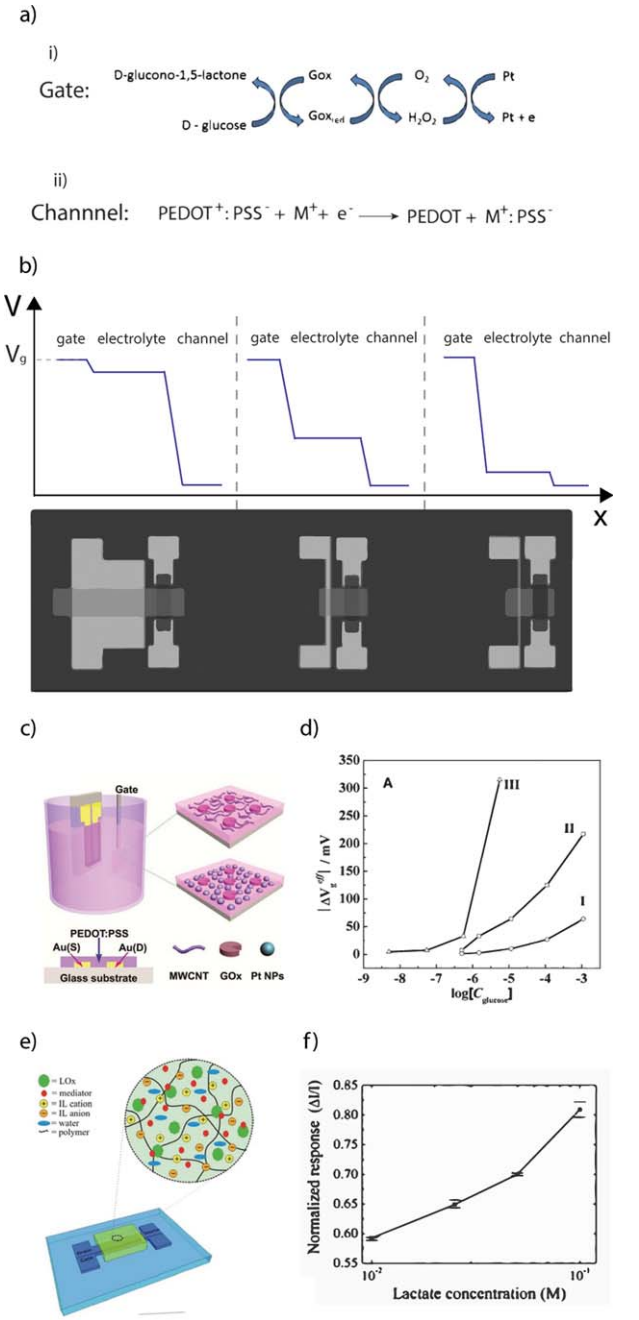

Figure 4. OECTs used as enzymatic sensors: a. (i) transfer of electron from glucose to the gate through the biological reaction catalyzed by glucose oxidase and (ii) dedoping mechanism of PEDOT:PSS at the channel b. Drop of potential at the interfaces and its dependence on the gate/channel size ratio. (b, is reproduced and modified from [57] with permission from [Wiley Online Library]) c. Schematic layout of an OECT glucose sensor with the gate modified with Pt–NPs, MWCTS, and GOx. d. The dependence of $\Delta V_{g,eff}$ as a function of log[$C_{glucose}$] for CHIT/GOx/Pt (line I), MWCNT-CHIT/GOx/Pt (line II) and CHIT/GOx/Pt-NPs/Pt (line III) gate electrodes. (c, d are reproduced from [58] with permission from [Wiley–VCH]). e. Schematic layout of an OECT lactate sensor with solid state ionogel electrolyte. f. Normalized response of the OECT vs. lactate concentration. (e, f are reproduced from [59] with permission from [RSC Publishing]). [Color figure can be viewed in the online issue, which is available at wileyonlinelibrary.com.]

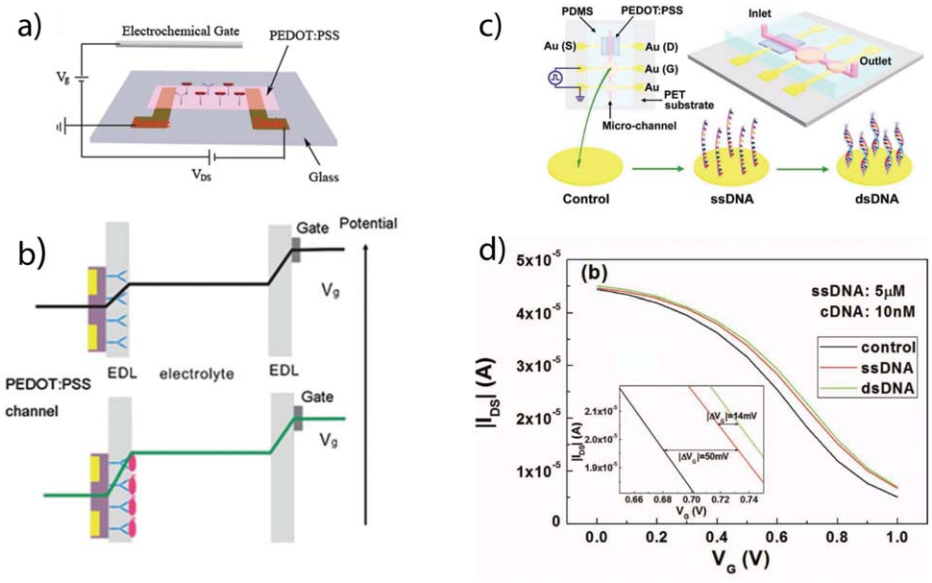

Figure 5. OECTs as immunosensors and nucleotide sensors: a. Schematic of an *E. coli* O157:H7 sensor based on an OECT. b. Schematic diagram of potential drops in the EDLs, including the channel/electrolyte and electrolyte/gate interfaces, in the OECT before and after the immobilization of *E. coli* O157:H7 on the PEDOT:PSS surface. (a, b, reproduced from [72], with permission from [RSC Publishing]) c. Schematic of an OECT integrated in a flexible microfluidic system, which is characterized before and after the modification and the hybridization of DNA on the surface of Au gate electrode. d. Transfer characteristics of OECTs measured in microfluidic channels before and after the immobilization and the hybridization of DNA on Au gate electrodes. $V_{ds} = -0.1$ V. The inset shows the horizontal shifts of the transfer curves. (c, d, reproduced from [73], with permission from [Wiley Online Library]). [Color figure can be viewed in the online issue, which is available at wileyonlinelibrary.com.]

of enzyme conformation and function. For this application, Yang and coworkers dissolved both the mediator and the enzyme in the RTIL and drop casted on top of a hydrophobic virtual well. The glucose sensor showed sensitivities in the micromolar range. Subsequently, Khodagholy *et al.*,[59] combining ionic liquids with cross linkable polymers, developed an OECT lactate sensor integrated with a solid state electrolyte. The ionic liquid gel electrolyte included: lactate oxidase and the ferrocene mediator for sensing, RTIL for its high ionic conductivity and for the stabilization of enzyme's conformation, and photo-crosslinkable monomer and photo-initiator for creating the solid state electrolyte [Figure 5(e)]. Drop-casting and subsequent polymerization under UV light resulted in a gel-like electrolyte. Figure 5(f) shows the normalized response of the OECT for a concentration range of lactate that exists in human sweat. This type of device was proposed as a wearable long term sensor for continuous monitoring of lactate levels in athletes. Finally, OECTS have been integrated with microfluidics for the fabrication of multianalyte sensors: Yang *et al.*,[27] demonstrated surface directed microfluidic that uses capillarity forces to drive a sample consisting of glucose and lactate to an array of OECTs for simultaneous measurement of glucose and lactate.

OECTs as Immunosensors/Nucleotide Sensors

OECTs can detect the presence of cells and biomolecules. Specifically, when a cell is in the proximity of an OECT channel, its membrane is polarized, resulting in an additional potential. The cause for the polarization of the cell is the potential difference between the channel and cell.[74] This additional potential shifts the effective gate voltage to lower values affecting the dedoping of the channel. Using this principle, He *et al.*,[72] have fabricated an OECT that detects the presence of a pathogenic strain of *E. coli*. In more detail, an immobilization step of the anti-*E. coli* antibody took place through biofunctionalization of the OECT channel [Figure 5(a)]. The *E. coli* bacteria were then captured through antibody antigen interactions. When the bacteria are in a low ionic concentration media they exhibit a negative charge in their membrane, thus immobilized bacteria on top of the OECT channel form a negatively charged layer. Consequently, on application of a gate voltage the negatively charged layer of bacteria attracts positive ions in the electrolyte, resulting in a shift of the $V_{g,eff}$ to lower values (logarithmically proportional to the concentration), which means that fewer ions are dedoping the channel or a higher voltage has to be applied to dedope the same magnitude of current in the absence of bacteria [Figure 5(b)]. The sensitivity of the device depends additionally on the ionic strength of the electrolyte, showing increasing sensitivity when the concentration of the electrolyte decreases.[13] This can limit the performance of the sensor in high ionic concentration electrolytes. Similarly, Kim *et al.*,[75] fabricated an OECT-based immunosensor for prostate specific antigen (PSA), by immobilizing a PSA specific antibody on the channel. The shift of the $V_{g,eff}$ to the channel is proportional to the captured PSA antigen concentration. A secondary antibody conjugated with Au nanoparticles was then used in a typical sandwich-ELISA format, thereby resulting in an increased sensitivity, mostly likely due to the fact that Au–NPs are negatively charged in suspension.

Finally, an OECT DNA sensor has been developed by Lin *et al.*,[73] Figure 5(c) shows the layout of the device, which consists of an OECT with integrated microfluidics on top of a

flexible polyethylene terephthalate substrate. Single stranded DNA was immobilized on the gate, with a second gate used as a control. Figure 5(d) shows a transfer curve, in which the gate voltage needed to dedope the channel shifts to higher values after immobilization and hybridization of the complementary DNA strand. The mechanism of sensing is as described above; owing to its charge, the DNA affects the capacitance at the interface between gate and electrolyte, and thus shifts $V_{g,eff.}$ A similar mechanism was also shown by Liao *et al.*, for the detection of diatoms, a type of algae found in sea water.[76] An interesting observation was that PEDOT:PSS appeared to promote diatom growth when compared with simple glass slides.

OECT Coupled with Whole Cells for Electrophysiology

In this section, work related to the coupling of OECTs with live mammalian cells will be discussed, rather than individual biomolecules or macromolecules as in the previous section. This section has been split into two sections; integration with nonelectrogenic cells for monitoring toxicology/diagnostics, and, integration with electrogenic cells such as cardiomyocytes and neurons. In the former case, the OECT is used to measure a "passive" electrical property of the cells, whereas, in the latter, the OECT is measuring active electrical properties of the cells, with applications both *in vitro* for toxicology/diagnostics, but also *in vivo* for potential therapeutics.

Integration of OECTs with Nonelectrogenic Cells

The first report of OECTs with live mammalian cells was by Bolin *et al.* [77] Madin Darby canine kidney (MDCK) epithelial cells were seeded along the channel of an OECT and the device was used to bias the channel such that an electrochemical gradient was produced. Depending on the redox potential of discrete areas of the channel, differential cell adhesion was observed, illustrating the potential for CPs with electrically tuneable surface properties in controlling adhesion of cells. A nontrivial issue associated with this work was the demonstration by the authors that live cells grow and proliferate on CP devices, indicating the biocompatibility of the materials used. Long term stability of these devices in cell culture media has also been demonstrated.[78] Subsequent integration of OECTs with live cells have focused on the sensitivity of the devices to changes in biological ion flux, a parameter which can be used for monitoring the integrity of mammalian cells, as the flow of ions is tightly regulated in tissues and dysregulation is often a sign of disease or dysfunction. In particular, OECTs have been used as an alternative technology for sensing barrier tissue integrity, monitoring variations in paracellular ion flux with state-of-the-art temporal resolution and high sensitivity. Barrier tissue is composed of epithelial or specialized endothelial cells whose role is to modulate ion flux between different bodily compartments. As this role is often compromised during toxic events, monitoring of this tissue is very interesting for diagnostics/toxicology. In a first instance, Jimison *et al.*,[79] integrated epithelial cells grown on filter supports with the OECT, using a model of the gastrointestinal tract Caco-2 cell line which is established as a barrier tissue model [Figure 6(a)]. This configuration is compatible with existing barrier tissue characterization and toxicology methods and protocols which frequently use filter supports as they mimic the polarized nature of the cells *in vivo* where they

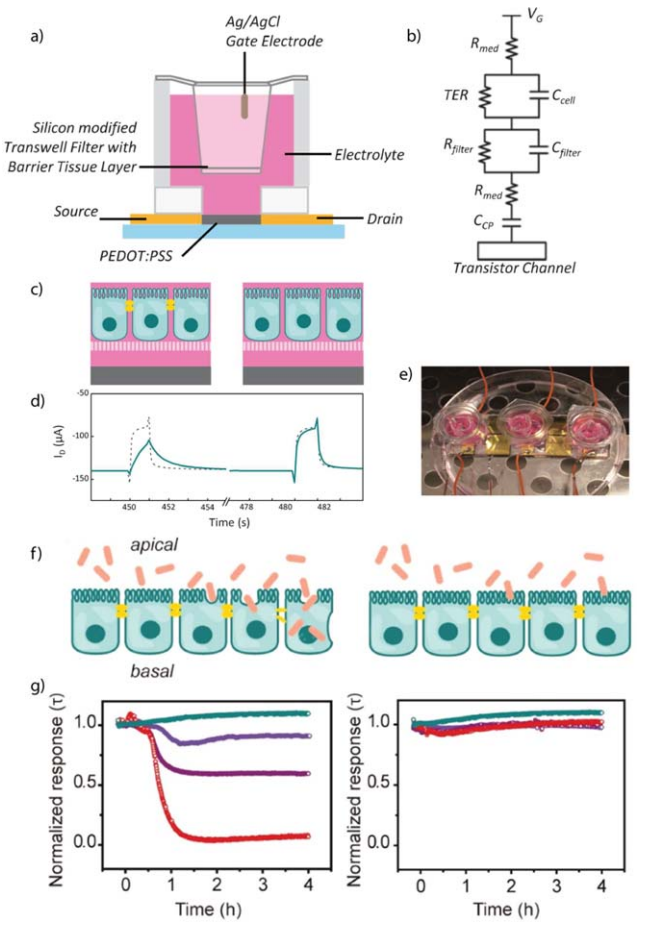

Figure 6. Barrier tissue integrity monitored with an OECT: a. layout of an OECT with an integrated barrier tissue, b. equivalent circuit describing ionic transport between gate electrode and transistor channel. TER refers to the transepithelial resistance of the cell layer, C_{cell} refers to the capacitance of the cell layer, R_{filter} and C_{filter} refer to the resistance and capacitance of the porous filter, respectively, R_{med} refers to the resistance of the media, and C_{cp} refers to the capacitance at the CP and electrolyte layer, c. cartoon showing polarized Caco-2 cells with tight junctions (left) and without (right), sitting on a porous cell culture membrane, above a PEDOT:PSS transistor channel. Tight junctions are shown in yellow. d. OECT I_d transient response with cells before (left) and after (right) the addition of 100 mM H_2O_2,(solid lines). OECT I_d response in the absence of cells is overlaid (dashed lines) (a, b, c, d, reproduced from [79], with permission from [Wiley Online Library]). e. Picture of the multiplex device shown on a Petri dish inside the cell-culture incubator. The cell culture insert is shown suspended in the plastic holder affixed to the glass slide. The Ag/AgCl gate electrode is shown immersed in the apical media, while source and drain cables are attached to their respective positions on the glass slide, f. cartoon illustrating infection with wildtype (WT) (left) and noninvasive *S. typhimurium* (right). g. Mean normalized response (τ) of the OECT in the presence of WT (left) and noninvasive *S. typhimurium* (right) at different MOI over 4 h, bacteria were added at $t = 0$. Noninfected represents OECT + cells with no added bacteria. Noninfected cells are in cyan, MOI: 10 in blue, MOI: 100 in purple, and MOI: 1000 in red. (e, f, g, reproduced from [80], with permission from [Wiley Online Library]). [Color figure can be viewed in the online issue, which is available at wileyonlinelibrary.com.]

separate different functional compartments (e.g., gastrointestinal tract from blood stream). The OECT ionic circuit on the addition of barrier tissue is shown schematically in Figure 6(b), with the cell layer represented as a resistor and capacitor in parallel. In this way, the OECT uses the ionic to electronic transduction to measure changes in the impedance of the ionic circuit. Application of a positive gate voltage V_g leads cations from the electrolyte, in this case cell culture media, into the CP channel thus dedoping it. The transient response, which gives the time of how fast the channel will be dedoped, can be quantified by the time constant ($\tau = RC$). The τ depends on the capacitance of the channel and the resistance of the electrolyte. The presence of the barrier tissue modifies the ionic flux, due to the addition of additional capacitor and resistor [Figure 6(b)] and the drain current by inducing a slow response and thus an increase in the τ.[42]

The disruption of barrier tissue [illustrated schematically in Figure 6(c)], related to the destruction of protein complexes between the cells, was also demonstrated on addition of hydrogen peroxide (H_2O_2), a known toxin. Figure 6(d) illustrates the high temporal resolution of the OECT in monitoring barrier tissue disruption, from one pulse to the next. Monitoring of the I_d response to the gate voltage was normalized as a function of time in the presence of both H_2O_2 and a second toxin, ethanol, and shown to have greater sensitivity than traditional methods. The effect of EGTA (Ethylene glycol-bis(beta-aminoethyl ether)-N,N,N′,N′-tetra acetic acid) known to affect paracellular ion transport pathways and trans epithelial resistance of cells has also been demonstrated with the OECT.[81] Dose dependent responses to addition of EGTA were detected and validated against existing commercially available electrical impedance spectroscopy shown significant advantages of the OECT in terms of temporal resolution. A visual demonstration of the OECT fabrication and operation for monitoring barrier tissue disruption by EGTA has also been reported.[82]

For nonacute diagnostics applications where time scales for readouts exceed minutes and may actually extend to days or even weeks, not only the stability of the sensor, but also the environmental conditions for measurement must be required. To test the stability of the OECT and assess suitability for long term measurements of an OECT, Tria *et al.,* transitioned the device to a format compatible with operation in physiological conditions, and to cope with the many varying parameters inherent to biological systems, the number of devices operated simultaneously was scaled-up [Figure 6(e)].[82] This system was used to successfully monitor the kinetics of integrity of the same gastrointestinal model after infection with the pathogenic organism *Salmonella typhimurium* [illustrated in Figure 6(f)], while a nonpathogenic *Salmonella* bacterium showed no response regardless of the concentration added [Figure 6(g)]. The experiment was also carried out in milk, a complex matrix containing many different compounds including proteins and fats; however, the OECT operation and detection of *Salmonella typhimurium* remained robust, unlike a leading commercially available alternative based on electrical impedance scanning using stainless steel electrodes.

OECTs show promise for applications requiring rapid and dynamic detection of variations in ion flow. The examples cited up until now have involved integration of the cells on a filter, physically separated from the device by the electrolyte, using a top-gate format. Another approach to measure the integrity of cells is to seed the cells directly on device, either with a top-gate format, or with a side-gate. This former principle was used by Lin *et al.,* and the device was shown to be able to detect cell attachment and cell detachment by shifting the $V_{g,eff}$ values, via a mechanism similar to that used by Yan and coworkers for detecting antibody/DNA binding.[83] Again the stable operation of the OECT in cell culture medium was confirmed, as well as the ability to support cell growth, in this case two cell lines: human esophageal squamous epithelial cancer cells and fibroblasts. In a similar configuration, Yao *et al.*,[84] show the integration of human airway epithelial cells with the OECT. Cells were seeded directly on an OECT array, however, the cells directly above the PEDOT:PSS channel are postulated to be suspended over the channel with a gap formed below [Figure 7(a)]. The authors investigated the dose response of transepithelial ion transport to forskolin, an agonist which causes opening of the cystic fibrosis transmembrane conductance regulator (CFTR) channel [Figure 7(b)], a major contributor to transcellular ion transport. The transport of Na^+ ions from the basolateral compartment to the apical compartment, result in a change in the channel current, which the authors convert to an effective gate voltage change. Ramuz *et al.*, combined optical and electronic sensing of epithelial cells using OECTs with both the gate and the channel in the same plane, both consisting of PEDOT:PSS.[85] This circumvents an issue for long term operation of devices using Ag/AgCl electrodes which were demonstrated to be toxic to live cells for periods >10 h.[82] MDCK I cells were seeded directly over an area comprising both the channel and the gate. The authors demonstrated the possibility for continuous measurements of ion flow in epithelial cells coupled with optical imaging of the cell layer on the device, thanks to the transparent nature of the PEDOT:PSS film [Figure 7(c)]. Further, the measured electrical signal is demonstrated to be due to tight junction-related barrier tissue formation and not to simple cell coverage as the presence of cells on the active area of the OECT does not change the transistor response to gate pulse voltage unless the cells present barrier tissue properties. A corollary of this work is that high resolution imaging of cells is possible on PEDOT:PSS films, not only in bright field mode, but also for fluorescence imaging [Figure 7(d)], highly valuable for definition of molecular mechanisms in biological systems.

OECT for Stimulation and Recording of Electrogenic Cells

Electrical stimulation and recording of nerve tissue and neural activity have provided valuable information about physiological and pathological functions of the body and brain. Typically, these recordings are performed with metal electrodes.[5] For example, the main technique to record cardiac activity, electrocardiography (ECG), uses electrodes in contact with the skin which provide information about the normal function or abnormalities of the heart. OECTs include advantages that can overcome many limitations in electrophysiology. First of all, the

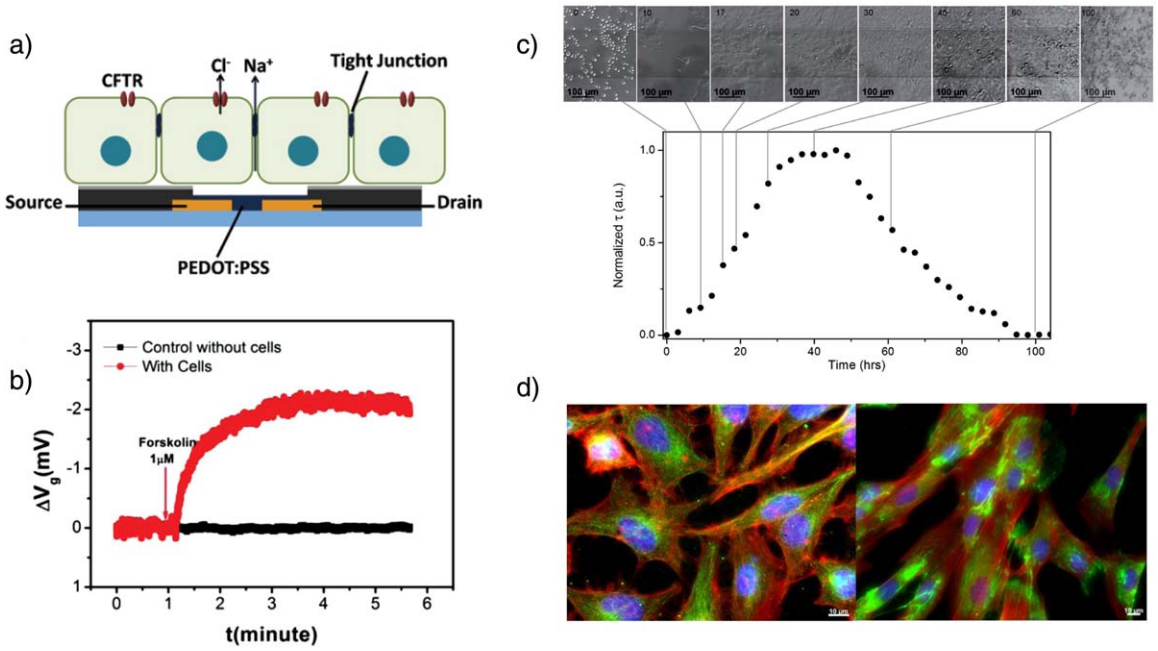

Figure 7. Non electrogenic cells in direct contact with OECTs: a. illustration of polarized Calu-3 cells with tight junction sitting on the PEDOT:PSS transistor channel of an OECT. b. In situ OECT response with (red) and without (black) Calu-3 cells on the addition of 1 μM CFTR agonist forskolin. Transistor channel current change was converted to effective gate voltage change. (a, b reproduced from [84], with permission from [Wiley Online Library]). c. Microoptical images of MDCK-I on top of the OECT channel area (the darker horizontal line in the middle of the picture corresponds to the PEDOT:PSS channel) and corresponding electrical characteristics with a measurement taken every 3 h. d. Illustrative example of high resolution fluorescence imaging possible on PEDOT:PSS devices. HeLa cells (left) and immortalized human fibroblasts (right) (c, d, reproduced from [85], with permission from [Wiley Online Library]). [Color figure can be viewed in the online issue, which is available at wileyonlinelibrary.com.]

low temperature fabrication of OECTs enables devices on flexible, biocompatible, and biodegradable substrates. Campana *et al.*,[86] fabricated OECTs on flexible, resorbable poly(L-lactide-co-glycolide substrates for ECG recordings. Figure 8(a) shows the layout of the measurements and the raw signal compared to the theoretical heart pulse. In this work, the gate of the OECT was placed directly on skin close to the heart at a constant positive potential (V_g = 0.5 V) relative to the ground potential of the body, while the transistor channel was placed on the forearm at a negative potential (V_d = −0.3 V) relative to the ground. Every heartbeat creates an additional potential which modulates the $V_{g,eff}$ seen by the channel and result in a clear dedoping of the channel. Conductive gels are usually used as an interface between the skin and channel to increase the adhesion for long–term measurements. Figure 8(b) shows how the fabrication of the device on a flexible substrate improves the contact with the skin which is desirable for recordings of freely moving subjects. Furthermore, the use of biodegradable materials can push to implantable devices that can be used for recording or stimulating electrogenic cells.

For the brain, there are three main electrophysiology recording techniques: electroencephalography (EEG) which utilizes electrodes in contact with the skin, electrocorticography (ECoG) which utilizes electrodes in contact with the surface of the brain, and stereoelectroencephalography (SEEG) which utilizes probes that penetrate deep in the brain.[88] Depending on the nature of the signal of interest, or the size of the neural population to be interrogated, or the invasiveness/goal of the measurement, EEG, ECG, or SEEG may be selected. Most of the electrodes currently used are relatively inflexible, anchored in the skull, and do not follow the movements of the brain. Moreover, the recording quality usually deteriorates over time, due to the tissue injury and reaction of the immune system to the electrode.[89] A primary challenge is to form a good contact with the brain. This can be achieved by using flexible electrodes that conform to the shape of the brain surface.[29] Other requirements are to obtain high quality and stable overtime recordings, that is, through the use of more biocompatible materials, and of course amplification of neuronal signals necessary to detect low magnitude signals of interest. As a proof of concept, Khodagholy *et al.*,[22] demonstrated implantable OECTs for ECoG recordings. A conformal device, consisting of integrated electrodes and OECTs array, was placed on the surface of the brain of an epileptic rat [Figure 8(c)]. The dimensions of the devices are on the order of few micrometers, fabricated on top of a 2 μm polymer substrate. Figure 8(d) shows that the signal to noise ratio of the OECT was far superior compared to the electrodes. Furthermore, the OECT could record low amplitude signals and fast signals from the interior of the brain that the electrodes were unable to detect, hitherto only recordable by depth probes (SEEG). Finally, a recent publication has demonstrated the use of an OECT to monitor cardiac rhythm, eye movement, and brain activity in a human volunteer [Figure 8(e,f)].[87] The device showed a high transconductance operation at low gate voltage,

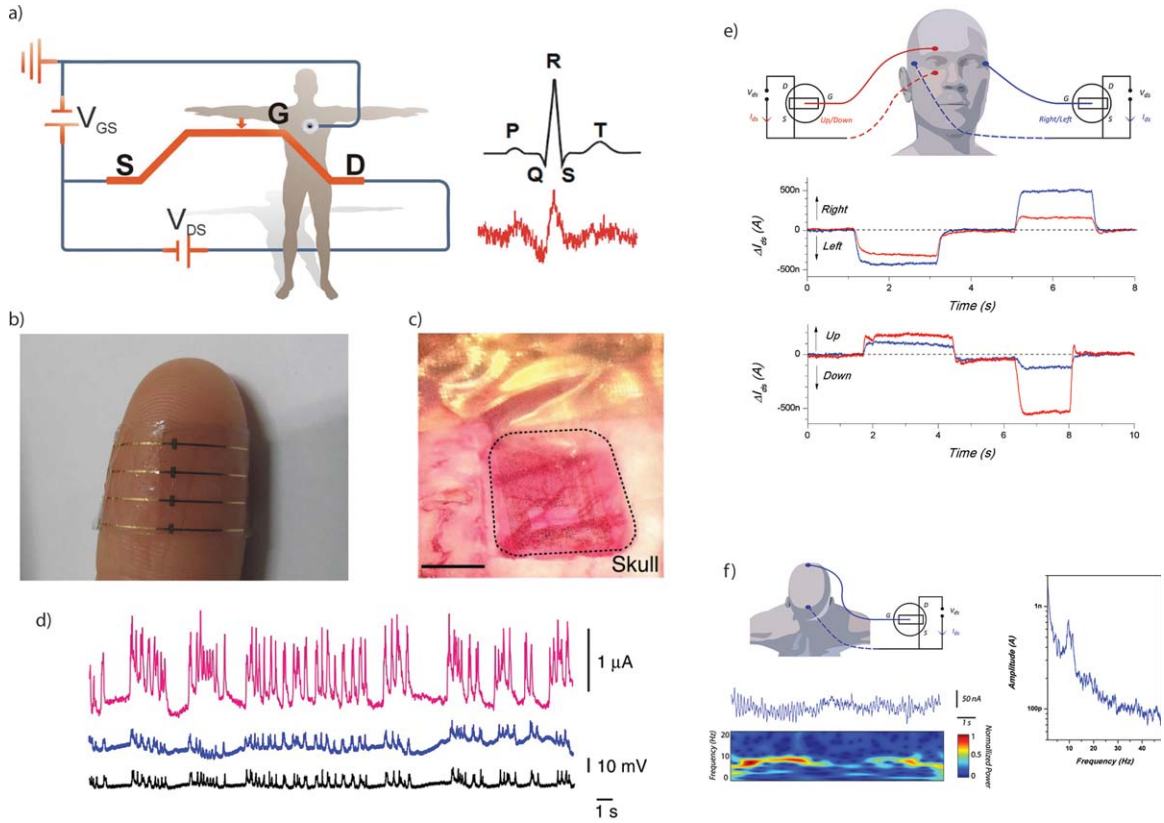

Figure 8. OECTs for measuring electrogenic cells: a. ECG recording with an OECT operated in direct contact with the skin. b. Photograph of the device showing its transparency and adaptability when attached to human skin. (a, b, reproduced from [86], with permission from [Wiley Online Library]). c. Optical micrograph of the ECoG probe placed over the somatosensory cortex, with the craniotomy surrounded by dashed lines. Scale bar, 1 mm. d. Recordings from an OECT (pink), a PEDOT:PSS surface electrode (blue) and an Ir-penetrating electrode (black). The transistor was biased with $V_d = -0.4$ V and $V_g = 0.3$ V, and the scale of 10 mV is for both surface and penetrating electrodes. Note the superior SNR of the OECT as compared with the surface electrode. (c, d, reproduced from [22], with permission from [Nature Publishing Group]). e. Wiring configuration chosen for the EOG measurement, recording of electrical activity during left/right eyeball movements, recording of electrical activity during up/down eyeball movements. Both up/down (red) and left/right (blue) activities are measured. f. Wiring configuration used for the EEG measurement, along with recording of spontaneous brain activity (top) showing the alpha rhythm, and associated time-frequency spectrogram (bottom), Fourier analysis of a 3 min recording. (e, f, reproduced from [87], with permission from [Wiley–VCH]). [Color figure can be viewed in the online issue, which is available at wileyonlinelibrary.com.]

which simplified the wiring, as it necessitated only one power supply to bias the drain.

CONCLUSIONS

Bioelectronics is a growing interdisciplinary field which aims to interface electronics and biology, improving current biomedical tools. The particular niche for organic electronic materials in integration with biological materials or use in biomedical applications comes from a host of beneficial properties unique to these materials in contrast to traditional electronic materials. The underlying notion of amplification, a prerequisite in biosensing, pushes toward active devices (transistors) rather than passive devices (electrodes). The OECT lies at the heart of this field principally because of the intimate nature of the interface with biological components, where the biological milieu comprises an integral part of the device, and ions from this milieu are the key to the operation mechanism of the OECT. Improved signal transduction and amplification are common themes in the research cited above, demonstrated repeatedly for the OECT in a wide variety of formats and applications. Stability is a highly valued characteristic for biosensing, and the OECT has been shown to operate stably in a variety of different electrolytes, including complex cell media, seawater, and even milk. Long term operation in these electrolytes on the scale of days to weeks has also been possible.

The OECT is a current to voltage transducer; small changes at the input ($\Delta V_{g,eff}$) result in big changes at the output (ΔI_d). OECTs exhibit high transconductance values, essentially high gain, and by tuning the geometry and the size of the channel, the transconductance and the time response can be optimized. Different modes of operation depend on how the effective gate voltage ($V_{g,eff}$) shifts. For example, the $V_{g,eff}$ can be modulated by changes in the resistance of the electrolyte, charge transfer to the gate, or sensing of an additional external ΔV_g signal. Using this principle, OECTs have been used as ion-sensors, enzymatic sensors, DNA sensors, immunosensors, and pathogen sensors. Further, OECTs have been integrated with individual cells, tissues, and even whole organs. Application dependent tuning is a

very important benefit of the use of CPs, which are amenable to chemical modification, biofunctionalization, and fabrication using a wide variety of techniques on different substrates. Compatibility with photolithographical techniques also facilitates fabrication of micron-scale devices, particularly interesting for monitoring of cells *in vitro* and *in vivo*, as well as for high-throughput device arrays.

Although considerable progress has been made in the past decade on the development of OECTs for biological applications, numerous challenges remain. These include the development and implementation of novel active materials (CPs) with improved properties in terms of conductivity, stability, patterning, resorbability, so forth. Another significant challenge lies in the fabrication of circuits for integrating sensors with multiplex miniaturized arrays, as well as integration of circuits that will potentially power, record, and transmit the recordings. Future applications for OECTs are expected to further exploit the beneficial properties of these devices, with significant potential in tissue engineering for *in vivo* applications. The first wave of industrial prototypes in the biomedical arena is anticipated imminently.

ACKNOWLEDGMENTS

The authors gratefully acknowledge funding from the European Research Council ERC-2010-StG Proposal No 258966 (IONOSENSE) as well as an ANRT doctoral fellowship (XS). The authors wish to thank Jonathan Rivnay for helpful comments and discussions.

REFERENCES

1. Berggren, M.; Richter-Dahlfors, A. *Adv. Mater.* **2007**, *19*, 3201.
2. Svennersten, K.; Larsson, K. C.; Berggren, M.; Richter-Dahlfors, A. *Biochim. Biophys. Acta* **2011**, *1810*, 276.
3. Owens, R.; Kjall, P.; Richter-Dahlfors, A.; Cicoira, F. *Biochim. Biophys. Acta* **2013**, *1830*, 4283.
4. Owens, R. M.; Malliaras, G. G. *MRS Bull.* **2010**, *35*, 449.
5. Buzsáki, G.; Anastassiou, C. A.; Koch, C. *Nat. Rev. Neurosci.* **2012**, *13*, 407.
6. Rivnay, J.; Owens, R. M.; Malliaras, G. G. *Chem. Mater.* **2014**, *26*, 679.
7. White, H. S.; Kittlesen, G. P.; Wrighton, M. S. *J. Am. Chem. Soc.* **1984**, *106*, 5375.
8. Khodagholy, D.; Rivnay, J.; Sessolo, M.; Gurfinkel, M.; Leleux, P.; Jimison, L. H.; Stavrinidou, E.; Herve, T.; Sanaur, S.; Owens, R. M.; Malliaras, G. G. *Nat. Commun.* **2013**, *4*, 2133.
9. Bernards, D. A.; Malliaras, G. G. *Adv. Funct. Mater.* **2007**, *17*, 3538.
10. Kim, S. H.; Hong, K.; Xie, W.; Lee, K. H.; Zhang, S.; Lodgeand, T. P.; Frisbie, C. D. *Adv. Mater. (Deerfield Beach, Fla.)* **2013**, *25*, 1822.
11. Crone, B.; Dodabalapur, A.; Gelperin, A.; Torsi, L.; Katz, H. E.; Lovinger, A. J.; Bao, Z. *Appl. Phys. Lett.* **2001**, *78*, 2229.
12. Magliulo, M.; Mallardi, A.; Mulla, M. Y.; Cotrone, S.; Pistillo, B. R.; Favia, P.; Vikholm-Lundin, I.; Palazzo, G.; Torsi, L. *Adv. Mater. (Deerfield Beach, Fla.)* **2013**, *25*, 2090.
13. Hammock, M. L.; Knopfmacher, O.; Naab, B. D.; Tokand, J. B. H.; Bao, Z. *ACS Nano* **2013**, *7*, 3970.
14. Torsi, L.; Magliulo, M.; Manoli, K.; Palazzo, G. *Chem. Soc. Rev.* **2013**, *42*, 8612.
15. Kergoat, L.; Piro, B.; Berggren, M.; Horowitz, G.; Pham, M.-C. *Anal. Bioanal. Chem.* **2012**, *402*, 1813.
16. Blaudeck, T.; Ersman, P. A.; Sandberg, M.; Heinz, S.; Laiho, A.; Liu, J.; Engquist, I.; Berggren, M.; Baumann, R. R. *Adv. Funct. Mater.* **2012**, *22*, 2939.
17. Basiricò, L.; Cosseddu, P.; Fraboni, B.; Bonfiglio, A. *Thin Solid Films* **2011**, *520*, 1291.
18. Basiricò, L.; Cosseddu, P.; Scidà, A.; Fraboni, B.; Malliaras, G. G.; Bonfiglio, A. *Org. Electron.* **2012**, *13*, 244.
19. Kaihovirta, N.; Mäkelä, T.; He, X.; Wikman, C.-J.; Wilén, C.-E.; Österbacka, R. *Org. Electron.* **2010**, *11*, 1207.
20. Nilsson, D.; Kugler, T.; Svensson, P.-O.; Berggren, M. *Sens. Actuators B* **2002**, *86*, 193.
21. Ersman, P. A; Nilsson, D.; Kawahara, J.; Gustafssonand, G.; Berggren, M. *Org. Electron.* **2013**, *14*, 1276.
22. Khodagholy, D.; Doublet, T.; Quilichini, P.; Gurfinkel, M.; Leleux, P.; Ghestem, A.; Ismailova, E.; Hervé, T.; Sanaur, S.; Bernard, C.; Malliaras, G. G. *Nat. Commun.* **2013**, *4*, 1575.
23. Shim, N. Y.; Bernards, D. A.; Macaya, D. J.; DeFranco, J. A.; Nikolou, M.; Owens, R. M.; Malliaras, G. G. *Sensors* **2009**, *9*, 9896.
24. Yang, S. Y.; Cicoira, F.; Byrne, R.; Benito-Lopez, F.; Diamond, D.; Owens, R. M.; Malliaras, G. G. *Chem. Commun.* **2010**, *46*, 7972.
25. Sessolo, M.; Khodagholy, D.; Rivnay, J.; Maddalena, F.; Gleyzes, M.; Steidl, E.; Buissonand, B.; Malliaras, G. G. *Adv. Mater.* **2013**, *25*, 2135.
26. Khodagholy, D.; Gurfinkel, M.; Stavrinidou, E.; Leleux, P.; Herve, T.; Sanaur, S. B.; Malliaras, G. G. *Appl. Phys. Lett.* **2011**, *99*, 163304.
27. Yang, S. Y.; Defranco, J. A.; Sylvester, Y. A.; Gobert, T. J.; Macaya, D. J.; Owens, R. M.; Malliaras, G. G. *Lab on a Chip* **2009**, *9*, 704.
28. Mabeck, J. T.; DeFranco, J. A.; Bernards, D. A.; Malliaras, G. G.; Hocdé, S.; Chase, C. *J. Appl. Phys. Lett.* **2005**, *87*, 013503.
29. Khodagholy, D.; Doublet, T.; Gurfinkel, M.; Quilichini, P.; Ismailova, E.; Leleux, P.; Herve, T.; Sanaur, S.; Bernard, C.; Malliaras, G. G. *Adv. Mater. (Deerfield Beach, Fla.)* **2011**, *268*.
30. Hamedi, M.; Forchheimer, R.; Inganäs, O. *Nat. Mater.* **2007**, *6*, 357.
31. Mattana, G.; Cosseddu, P.; Fraboni, B.; Malliaras, G. G.; Hinestroza, J. P.; Bonfiglio, A. *Org. Electron.* **2011**, *12*, 2033.
32. Muller, C.; Hamedi, M.; Karlsson, R.; Jansson, R.; Marcilla, R.; Hedhammar, M.; Inganas, O. *Adv. Mater.* **2011**, *23*, 898.
33. Heeger, A. J. *J. Phys. Chem. B* **2001**, *105*, 8475.
34. Heeger, A. J.; MacDiarmid, A. G.; Shirakawa, H. Royal Swedish Academy of Sciences; Stockholm, Sweden, **2000**.

35. Guimard, N. K.; Gomezand, N.; Schmidt, C. E. *Prog. Polym. Sci.* **2007**, *32*, 876.
36. Asplund, M.; Nybergand, T.; Inganas, O. *Polym. Chem.* **2010**, *1*, 1374.
37. Thompson, B. C.; Winther-Jensen, O.; Vongsvivut, J.; Winther-Jensen, B.; MacFarlane, D. R. *Macromol. Rapid Commun.* **2010**, *31*, 1293.
38. Heller, A. *J. Phys. Chem.* **1992**, *96*, 3579.
39. McQuade, D. T.; Pullen, A. E.; Swager, T. M. *Chem. Rev.* **2000**, *100*, 2537.
40. Jimison, L. H.; Rivnay, J.; Owens, R. M. In Organic Electronics; Wiley-VCH Verlag GmbH & Co. KGaA: Weinheim, Germany, **2013**, p 27–67.
41. Bongo, M.; Winther-Jensen, O.; Himmelberger, S.; Strakosas, X.; Ramuz, M.; Hama, A.; Stavrinidou, E.; Malliaras, G. G.; Salleo, A.; Winther-Jensen, B.; Owens, R. M. *J. Mater. Chem. B* **2013**, *1*, 3860.
42. Jimison, L. H.; Hama, A.; Strakosas, X.; Armel, V.; Khodagholy, D.; Ismailova, E.; Malliaras, G. G.; Winther-Jensen, B.; Owens, R. M. *J. Mater. Chem.* **2012**, *22*, 19498.
43. Strakosas, X.; Sessolo, M.; Hama, A.; Rivnay, J.; Stavrinidou, E.; Malliaras, G. G.; Owens, R. M. *J. Mater. Chem. B* **2014**, *2*, 2537.
44. Stavrinidou, E.; Leleux, P.; Rajaona, H.; Khodagholy, D.; Rivnay, J.; Lindau, M.; Sanaur, S.; Malliaras, G. G. *Adv. Mater. (Deerfield Beach, Fla.)* **2013**, *25*, 4488.
45. Simon, D. T.; Kurup, S.; Larsson, K. C.; Hori, R.; Tybrandt, K.; Goiny, M.; Jager, E. W. H.; Berggren, M.; Canlon, B.; Richter-Dahlfors, A. *Nat. Mater.* **2009**, *8*, 742.
46. Isaksson, J.; Kjall, P.; Nilsson, D.; Robinson, N.; Berggren, M.; Richter-Dahlfors, A. *Nat. Mater.* **2007**, *6*, 673.
47. Tybrandt, K.; Forchheimerand, R.; Berggren, M. *Nat. Commun.* **2012**, *3*, 871.
48. Rivnay, J.; Leleux, P.; Sessolo, M.; Khodagholy, D.; Hervé, T.; Fiocchi, M.; Malliaras, G. G. *Adv. Mater. (Deerfield Beach, Fla.)* **2013**, *25*, 7010.
49. Bernards, D. A.; Malliaras, G. G.; Toombes, G. E. S.; Gruner, S. M. *Appl. Phys. Lett.* **2006**, *89*, 053505.
50. Lin, P.; Yanand, F.; Chan, H. L. W. *ACS Appl. Mater. Interfaces* **2010**, *2*, 1637.
51. Svensson, P. -O.; Nilsson, D.; Forchheimer, R.; Berggren, M. *Appl. Phys. Lett.* **2008**, *93*, 203301.
52. Sessolo, M.; Rivnay, J.; Bandiello, E.; Malliaras, G. G.; Bolink, H. J. *Adv. Mater.* **2014**, *26*, 4803.
53. Tarabella, G.; Balducci, A. G.; Coppedè, N.; Marasso, S.; D'Angelo, P.; Barbieri, S.; Cocuzza, M.; Colombo, P.; Sonvico, F.; Moscaand, R.; Iannotta, S. *Biochim. Biophys. Acta* **2013**, *1830*, 4374.
54. Tarabella, G.; Nanda, G.; Villani, M.; Coppedè, N.; Mosca, R.; Malliaras, G. G.; Santato, C.; Iannotta, S.; Cicoira, F. *Chem. Sci.* **2012**, *3*, 3432.
55. Mousavi, Z.; Ekholm, A.; Bobacka, J.; Ivaska, A. *Electroanalysis* **2009**, *21*, 472.
56. Linand, P.; Yan, F. *Adv. Mater. (Deerfield Beach, Fla.)* **2012**, *24*, 34.
57. Cicoira, F.; Sessolo, M.; Yaghmazadeh, O.; DeFranco, J. A.; Yangand, S. Y.; Malliaras, G. G. *Adv. Mater. (Deerfield Beach, Fla.)* **2010**, *22*, 1012.
58. Tang, H.; Yan, F.; Lin, P.; Xuand, J.; Chan, H. L. W. *Adv. Funct. Mater.* **2011**, *21*, 2264.
59. Khodagholy, D.; Curto, V. F.; Fraser, K. J.; Gurfinkel, M.; Byrne, R.; Diamond, D.; Malliaras, G. G.; Benito-Lopez, F.; Owens, R. M. *J. Mater. Chem.* **2012**, *22*, 4440.
60. Nishizawa, M.; Matsue, T.; Uchida, I. *Anal. Chem.* **1992**, *64*, 2642.
61. Zhu, Z.-T.; Mabeck, J. T.; Zhu, C.; Cady, N. C.; Batt, C. A.; Malliaras, G. G. *Chem. Commun.* **2004**, 1556.
62. Bernards, D. A.; Macaya, D. J.; Nikolou, M.; DeFranco, J. A.; Takamatsu, S.; Malliaras, G. G. *J. Mater. Chem.* **2008**, *18*, 116.
63. Macaya, D. J.; Nikolou, M.; Takamatsu, S.; Mabeck, J. T.; Owens, R. M.; Malliaras, G. G. *Sens. Actuators B: Chem.* **2007**, *123*, 374.
64. Tang, H.; Lin, P.; Chanand, H. L. W.; Yan, F. *Biosens. Bioelectron.* **2011**, *26*, 4559.
65. Tarabella, G.; Pezzella, A.; Romeo, A.; D'Angelo, P.; Coppedè, N.; Calicchio, M.; d'Ischia, M.; Moscaand, R.; Iannotta, S. *J. Mater. Chem. B* **2013**, *1*, 3843.
66. Coppede, N.; Tarabella, G.; Villani, M.; Calestani, D.; Iannotta, S.; Zappettini, A. *J. Mater. Chem. B* **2014**, *2*, 5620.
67. Tarabella, G.; Santato, C.; Yang, S. Y.; Iannotta, S.; Malliaras, G. G.; Cicoira, F. *Appl. Phys. Lett.* **2010**, *97*, 123304.
68. Yaghmazadeh, O.; Cicoira, F.; Bernards, D. A.; Yang, S. Y.; Bonnassieux, Y.; Malliaras, G. G. *J. Polym. Sci. Part B: Polym. Phys.* **2011**, *49*, 34.
69. Liao, C.; Zhang, M.; Niu, L.; Zheng, Z.; Yan, F. *J. Mater. Chem. B* **2013**, *1*, 3820.
70. Kergoat, L.; Piro, B.; Simon, D. T.; Pham, M.-C.; Noël, V.; Berggren, M. *Adv. Mater. (Deerfield Beach, Fla.)* **2014**, *26*, 5658.
71. Lee, K. H.; Kang, M. S.; Zhang, S.; Gu, Y.; Lodgeand, T. P.; Frisbie, C. D. *Adv. Mater. (Deerfield Beach, Fla.)* **2012**, *24*, 4457.
72. He, R.-X.; Zhang, M.; Tan, F.; Leung, P. H. M.; Zhao, X.-Z.; Chan, H. L. W.; Yang, M.; Yan, F. *J. Mater. Chem.* **2012**, *22*, 22072.
73. Lin, P.; Luo, X.; Hsing, I. M.; Yan, F. *Adv. Mater. (Deerfield Beach, Fla.)* **2011**, *23*, 4035.
74. Lin, P.; Yan, F.; Yu, J.; Chan, H. L.; Yang, M. *Adv. Mater.* **2010**, *22*, 3655.
75. Kim, D.-J.; Lee, N.-E.; Park, J.-S.; Park, I.-J.; Kim, J.-G.; Cho, H. J. *Biosens. Bioelectron.* **2010**, *25*, 2477.
76. Liao, J.; Lin, S.; Liu, K.; Yang, Y.; Zhang, R.; Du, W.; Li, X. *Sens. Actuators B: Chem.* **2014**, *203*, 677.
77. Bolin, M. H.; Svennersten, K.; Nilsson, D.; Sawatdee, A.; Jager, E. W. H.; Richter-Dahlfors, A.; Berggren, M. *Adv. Mater.* **2009**, *21*, 4379.
78. Khodagholy, D.; Doublet, T.; Quilichini, P.; Gurfinkel, M.; Leleux, P.; Ghestem, A.; Ismailova, E.; Herve, T.; Sanaur, S.; Bernard, C.; Malliaras, G. G. *Nat. Commun.* **2013**, *4*, 1575.

79. Jimison, L. H.; Tria, S. A.; Khodagholy, D.; Gurfinkel, M.; Lanzarini, E.; Hama, A.; Malliaras, G. G.; Owens, R. M. *Adv. Mater.* **2012**, *24*, 5919.

80. Tria, S. A.; Ramuz, M.; Huerta, M.; Leleux, P.; Rivnay, J.; Jimison, L. H.; Hama, A.; Malliaras, G. G.; Owens, R. M. *Adv. Health. Mater.* **2014**, *3*, 1053.

81. Tria, S.; Jimison, L. H.; Hama, A.; Bongo, M.; Owens, R. M. *Biosensors (Basel)* **2013**, *3*, 44.

82. Tria, S. A.; Ramuz, M.; Jimison, L. H.; Hama, A.; Owens, R. M. *J. Vis. Exp.* **2014**, e51102.

83. Lin, P.; Yan, F.; Yu, J. J.; Chan, H. L. W.; Yang, M. *Adv. Mater.* **2010**, *22*, 3655.

84. Yao, C.; Xie, C.; Lin, P.; Yan, F.; Huang, P.; Hsing, I. M. *Adv. Mater.* **2013**, *25*, 6575.

85. Ramuz, M.; Hama, A.; Huerta, M.; Rivnay, J.; Leleux, P.; Owens, R. M. *Adv. Mater.* **2014**, *26*, 7083.

86. Campana, A.; Cramer, T.; Simon, D. T.; Berggren, M.; Biscarini, F. *Adv. Mater. (Deerfield Beach, Fla.)* **2014**, *26*, 3874.

87. Leleux, P.; Rivnay, J.; Lonjaret, T.; Badier, J. M.; Benar, C.; Herve, T.; Chauvel, P.; Malliaras, G. G. *Adv. Health. Mater.* to appear. DOI 10.1002/adhm.201400356 **2014**.

88. Jasper, H. H.; Arfel-Capdeville, G.; Rasmussen, T. *Epilepsia* **1961**, *2*, 130.

89. Gilletti, A. Muthuswamy, J. *J. Neural. Eng.* **2006**, *3*, 189.